DOI:10.1158/0008-5472.CAN-10-2638

Cancer Research

Coexpression of *Oct4* and *Nanog* Enhances Malignancy in Lung Adenocarcinoma by Inducing Cancer Stem Cell –Like Properties and Epithelial –Mesenchymal Transdifferentiation

Shih-Hwa Chiou, Mong-Lien Wang, Yu-Ting Chou, et al.

Cancer Res 2010;70:10433-10444. Published online December 14, 2010.

DOI:10.1158/0008-5472.CAN-10-2638

Cancer Research

Coexpression of *Oct4* and *Nanog* Enhances Malignancy in Lung Adenocarcinoma by Inducing Cancer Stem Cell–Like Properties and Epithelial–Mesenchymal Transdifferentiation

Shih-Hwa Chiou[1,2,3], Mong-Lien Wang[2], Yu-Ting Chou[4], Chi-Jen Chen[4], Chun-Fu Hong[4], Wang-Ju Hsieh[5], Hsin-Tzu Chang[2], Ying-Shan Chen[4], Tzu-Wei Lin[2], Han-Sui Hsu[6,7], and Cheng-Wen Wu[2,4,5,6]

Abstract

Epithelial–mesenchymal transition (EMT), a critical process of cancer invasion and metastasis, is associated with stemness property of cancer cells. Though *Oct4* and *Nanog* are homebox transcription factors essential to the self-renewal of stem cells and are expressed in several cancers, the role of *Oct4/Nanog* signaling in tumorigenesis is still elusive. Here microarray and quantitative real-time PCR analysis showed a parallel, elevated expression of *Oct4* and *Nanog* in lung adenocarcinoma (LAC). Ectopic expressions of *Oct4* and *Nanog* in LACs increased the percentage of *CD133*-expressing subpopulation and sphere formation, enhanced drug resistance, and promoted EMT. Ectopic expressions of *Oct4* and *Nanog* activated *Slug* and enhanced the tumor-initiating capability of LAC. Furthermore, double knockdown of *Oct4* and *Nanog* suppressed the expression of *Slug*, reversed the EMT process, blocked the tumorigenic and metastatic ability, and greatly improved the mean survival time of transplanted immunocompromised mice. The immunohistochemical analysis demonstrated that expressions of *Oct4*, *Nanog*, and *Slug* were present in high-grade LAC, and triple positivity of *Oct4/Nanog/Slug* indicated a worse prognostic value of LAC patients. Our results support the notion that the *Oct4/Nanog* signaling controls epithelial–mesenchymal transdifferentiation, regulates tumor-initiating ability, and promotes metastasis of LAC. *Cancer Res; 70(24); 10433–44. ©2010 AACR.*

Introduction

Lung cancer is one of the leading causes of cancer-related deaths worldwide (1). In particular, lung adenocarcinoma (LAC) is the most common histologic type. Its highly invasive and metastatic phenotypes are the major reasons for treatment failure and poor prognosis. Furthermore, a high failure rate and a low median survival rate are observed in patients undergoing chemoradiotherapy with recurrent, intractable LAC (2). To improve the patient survival, it is important to elucidate the regulatory mechanisms that control tumor-initiating and metastatic properties of LAC.

Authors' Affiliations: [1]Institute of Pharmacology, [2]Institute of Biochemistry and Molecular Biology, [5]Institute of Microbiology and Immunology, and [6]Institute of Clinical Medicine National, Yang Ming University, Taipei, Taiwan; [4]Institute of Biomedical Science, Academia Sinica, Taipei, Taiwan; [3]Department of Medical Research and Education and [7]Department of Surgery, Taipei Veterans General Hospital, Taipei, Taiwan

Note: Supplementary data for this article are available at Cancer Research Online (http://cancerres.aacrjournals.org/).

S.-H. Chiou, M.-L. Wang, and Y.-T. Chou contributed equally to this work.

Corresponding Author: Cheng-Wen Wu, Institute of Biochemistry and Molecular Biology, National Yang Ming University, No.155, Sec.2, Li-Nong St., Peitou, Taipei 112, Taiwan. Phone: 886-228267919; Fax: 886-228236518. E-mail: cwwu@ym.edu.tw

doi: 10.1158/0008-5472.CAN-10-2638

Self-renewal and pluripotency are the central features in the definition of embryonic stem cells (ESC), in which *Oct4* and *Nanog* play a key role in the maintenance of these processes (3, 4). *Oct4*, a member of the Pit-Oct-Unc (POU) transcription factor family, is essential to maintain self-renewal and is normally found in totipotent or pluripotent stem cells of pregastrulation embryos (3, 5). *Nanog*, a downstream target of *Oct4*, contributes to cell fate determination of the pluripotent inner cell mass during embryonic development (6) and its function requires the continued presence of *Oct4* (7). *Oct4* and *Nanog* have been suggested as 1 of 4 defined factors that render the reprogramming capability of adult cells into germline-competent–induced pluripotent stem cells (8–10). Previous studies also showed that mouse pulmonary stem cells endogenously express *Oct4* (11). *Oct4* was demonstrated to participate in tumorigenicity and malignancy of lung cancers (12). The expression of *Oct4* has further been shown in human breast cancer stem-like cells, implicating its involvement in self-renewal and tumorigenesis via activating its downstream target genes (13). Similar to *Oct4*, immunohistochemical analysis of colorectal tumor samples showed that overexpression of *Nanog* was strongly correlated with poor prognosis, lymph node metastasis, and Dukes classification of colorectal cancer (14). Recently, both *Oct4* and *Nanog* transcripts were consistently detected in human embryonic carcinomas, testicular germ cell tumors, seminomas, and bladder carcinomas (15–18). Furthermore, coexpression of *Oct4* and *Nanog* is associated with pancreatic carcinogenesis (19) and is

DOI:10.1158/0008-5472.CAN-10-2638

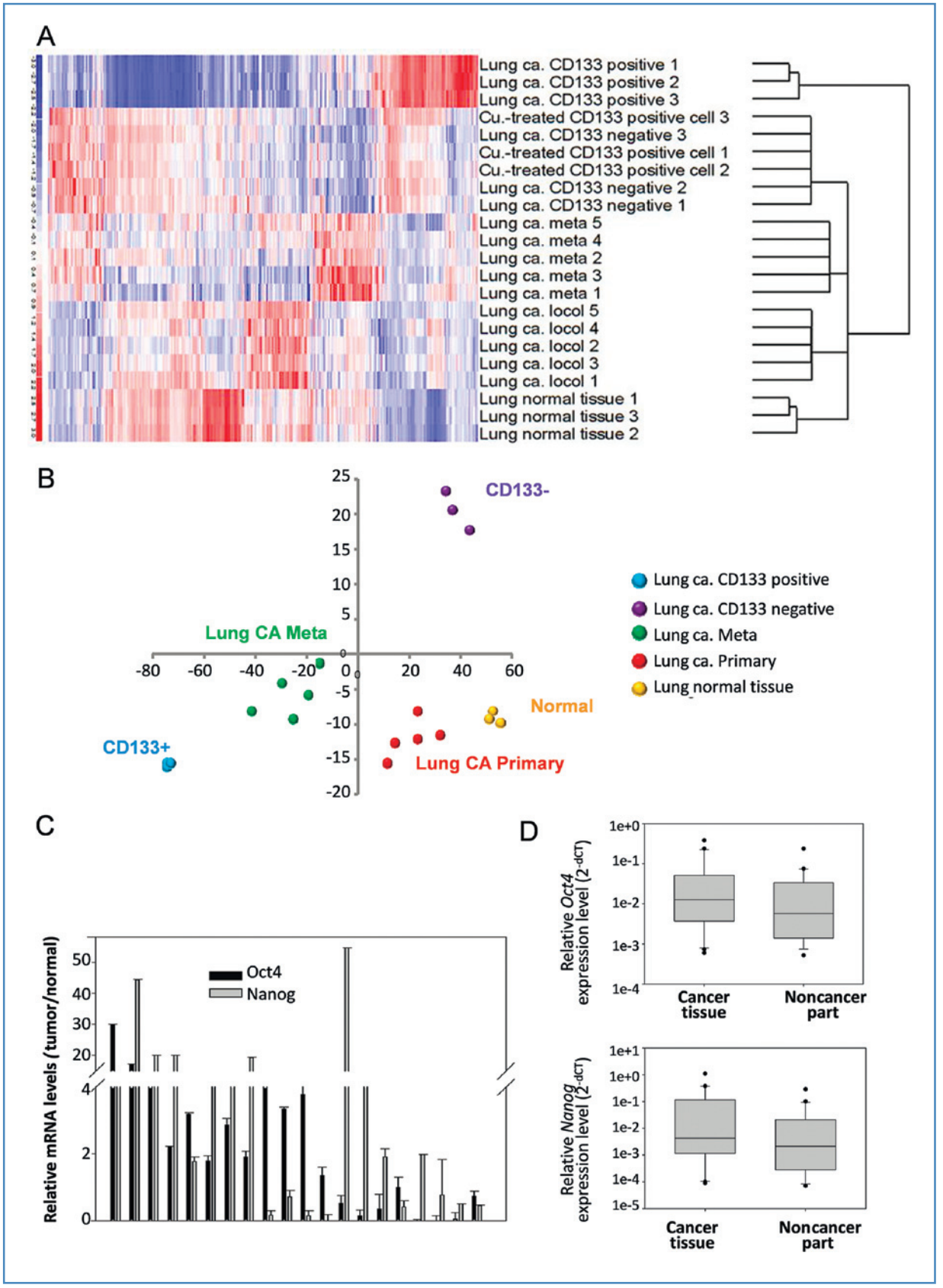

DOI:10.1158/0008-5472.CAN-10-2638

negatively correlated with the survival prognosis of oral squamous cell carcinoma patients (20). There is growing evidence of cross-talk and correlation between stemness pathways, tumor progression, and metastasis; the functional and mechanistic significance of the overexpressed stem cell markers in cancer, however, is still blurred and needs to be further clarified.

Epithelial–mesenchymal transition (EMT), a transdifferentiation program that converts adherent epithelial cells into individual migratory cells, is critical for embryonic development and the oncogenic progression of tumor cells (21, 22). The EMT process disrupts *E-cadherin* mediated cell–cell adhesion during embryonic development and changes the cell phenotype into a more loosely mesenchymal-like cell, leading to the invasion of extracellular matrix. Intensive studies revealed that transcriptional factors, such as *Snail*, *Slug*, and *Twist*, regulate EMT process (21, 22).

The recent study suggested that EMT could promote the property of stemness in normal breast tissues as well as breast cancer cells (23). However, the detailed molecular mechanisms involved in the regulatory links between EMT and stem cell–related genes are still poorly understood. In this study, we discovered that both *Oct4* and *Nanog* are highly expressed in $CD133^+$ but not in $CD133^-$ LAC cells, suggesting a positive involvement of *Oct4*/*Nanog* signaling in tumorigenesis. We further investigate the roles of *Oct4* and *Nanog* in EMT process, cancer progression, and metastasis of lung cancer. We found a significant coexpression of *Oct4* and *Nanog* in high-grade and metastatic lesions of patients with LAC. Ectopic expression of *Oct4* and *Nanog* in A549 LAC cells increases tumor-initiating properties, induces EMT and drug resistance, and promotes metastasis. This report provides the evidence bridging the missing link between EMT and stemness pathways and suggests a mechanism by which the *Oct4*/*Nanog* stem cell signaling encourages tumor malignancy and metastasis of LAC cells.

Materials and Methods

Cell culture

A549 lung cancer cell line was obtained from the American Type Culture Collection before 2007 and tested positive for human origin and for the presence of EGFR expression in the current genetic analysis. A549 cells were grown in RPMI-1640 medium with 10% fetal bovine serum.

Virus generation and infection

Virus generation and infection were performed as described (24). Briefly, 2.2×10^6 HEK293T cells were seeded onto a 100-mm culture dish 1 day before transfection. Cells were cotransfected with 10 μg of the pLKO.1-based lentiviral vector, 9 μg of Δ8.9 plasmid, and 2.5 μg of vesicular stomatitis virus G protein plasmid. The medium was replaced with normal culture medium 24 hours later, and the virus-containing medium was collected 48 hours after transfection. Lentiviral infection was performed by adding virus solution to cells at the desired multiplicity of infection in the presence of 8 ng/mL polybrene. Puromycin selection was performed 24 hours after infection until all of the mock-transfected cells died. Surviving cells were pooled and cultured for further analysis.

Microarray analysis and bioinformatics

Total RNA extraction was performed as described (24). Extracted RNA was reverse transcribed with Superscript II RNase H-reverse transcriptase (Gibco BRL) to generate Cy3- and Cy5-labeled (Amersham Biosciences Co.) cDNA probes for the control and treated samples, respectively. The labeled probes were hybridized to a cDNA microarray containing 10,000 gene clone immobilized cDNA fragments. Fluorescence intensities of Cy3 and Cy5 targets were measured and scanned separately using a GenePix 4000B Array Scanner (Axon Instruments). Data analysis was performed using GenePix Pro 3.0.5.56 (Axon Instruments) and GeneSpring GX 7.3.1 software (Agilent). The average linkage distance was used to assess the similarity between 2 groups of gene expression profiles as described below. The difference in distance between 2 groups of sample expression profiles to a third was assessed by comparing the corresponding average linkage distances [the mean of all pairwise distances (linkages) between members of the 2 groups concerned]. The error of such a comparison was estimated by combining the standard errors (the standard deviation of pairwise linkages divided by the square root of the number of linkages) of the average linkage distances involved. Classical multidimensional scaling was performed using the standard function of the R program to provide a visual impression of how the various sample groups are related (25).

Sphere formation assay

Cells were plated in 24-well plates (Falcon; BD) at a density of 5,000 viable cells/mL and grown in a serum-free Dulbecco's modified Eagle medium (DMEM; Sigma), supplemented with N2 plus media supplement (Invitrogen), 20 ng/mL of EGF and 20 ng/mL of bFGF (Invitrogen), and 4 μg/mL of heparin (Sigma). Cells were further allowed to grow for 12 days, and the numbers of spheres were counted by microscope.

Patients and tissue samples

LAC and adjacent nontumorous lung tissues were obtained at the time of surgery from 20 patients in Taipei Medical University Hospital and granted by the Institutional Review Board protocol number 010804. All patients gave their informed consent, and the ethics and scientific committees

Figure 1. Microarray analysis reveals key stemness-regulated transcriptomes in LAC. A, gene expression microarray analysis (gene tree) of the 987 genes that were differentially expressed in $CD133^+$ and $CD133^-$ LAC cells, metastatic and primary LAC, and normal lung tissues, as demonstrated by a hierarchical heat map. The changes of the expression of the 987 genes are presented as a log scale of the expression values provided by GeneSpring GX software. B, multidimensional scaling analysis illustrates the average lineage transcriptome distances between primary, metastatic LAC tissues, $CD133^-$, and $CD133^+$ cells. C, total RNA from 20 pairs of primary LAC and matching nontumorous lung tissues was analyzed for *Oct4* and *Nanog* mRNA expression by quantitative real-time PCR. D, the relative mRNA levels of *Oct4* and *Nanog* from the same patient were composed together and each bar represents the relative levels of *Oct4* and *Nanog* in LAC versus adjacent nontumorous lung tissue. The results are means of 3 independent experiments ± SD.

DOI:10.1158/0008-5472.CAN-10-2638

of the participating institutions approved the study. Tumor types were determined according to WHO classification. At the time of surgery, all tissue samples were immediately flash-frozen in liquid nitrogen and stored at −80°C until use.

Xenograft tumorigenicity assay

Virus-infected A549 cells were harvested, washed with PBS, and resuspended in normal culture medium. A549 cells (1×10^6) infected with *Oct4*/*Nanog* or control vector were injected subcutaneously into the right and left side, respectively, of the flank region of 8-week-old male BALB/c nude mice (Rodent Model Resource Center). Tumors were measured with calipers the days after injection as indicated. All mice were anesthetized and killed by overdose with anesthetic on day 42 after injection. Subcutaneous tumors were surgically excised, weighed, and photographed.

Statistical analysis

The results are reported as mean ± SD. Statistical analysis was performed using Student's *t* test or a 1-way or 2-way analysis of variance (ANOVA) test followed by Tukey's test, as appropriate. $P < 0.05$ was considered to be statistically significant.

Results

Microarray analysis of stemness-related gene expression profiling and linkages in primary and metastatic tissues of LAC

Recent reports have demonstrated that tumors contain a small subpopulation of cells, termed cancer stem-like or cancer-initiating cells, which exhibit a self-renewal capacity and are responsible for tumor maintenance and metastasis (26). Eramo and colleagues demonstrated that the small population of lung cancer–initiating cells could be identified by the *CD133* surface marker (27). On the other hand, *Oct4* was shown to play a crucial role in maintenance of the *CD133*$^+$ lung cancer–initiating cells (12). We analyzed the genomic traits of lung cancer LC-*CD133*$^+$ and LC-*CD133*$^-$ cells using gene expression microarray (Fig. 1A; Supplementary Tables S2, S3). To gain more insights into the functional consequences from differential gene expression patterns and to provide quantitative evidence, signature genes were subjected into the Gene Ontology database search to find statistically represented functional groups. The gene ontology categories of biological processes statistically represented ($P < 0.01$) among sphere-enriched genes are shown in Fig. 1A. The predominant processes upregulated in LC-*CD133*$^+$ include those pertaining to mitosis, nuclear division, and cell-cycle regulation (Supplementary Table S2a). In contrast, the downregulated genes in LC-*CD133*$^+$ include those related to immune responses, cell-to-cell adhesion, and cell biological adhesion (Supplementary Table S2b). Multidimensional scaling analysis showed that the gene expression pattern of LC-*CD133*$^+$ was closer to that of metastatic lesion of LAC, but far from that of LC-*CD133*$^-$ cells or primary lesion of LAC (Fig. 1B). In contrast, the gene signature of LC-*CD133*$^-$ was closer to that of primary lesion of LAC (Fig. 1B). Interestingly, the microarray analysis showed that the expression levels of ESC-specific genes, *Oct4* and *Nanog*, were significantly upregulated in LC-*CD133*$^+$ and metastatic lesion of LAC compared to LC-*CD133*$^-$ or primary lesion of LAC ($P < 0.001$; Supplementary Table S3a). Twenty pairs of LAC and corresponding adjacent nontumorous lung tissues were subjected to quantitative real-time PCR analysis. The levels of *Oct4* and *Nanog* RNA in the 20 LAC tissues were measured and represented as related levels compared to their adjacent nontumorous lung tissue (Fig. 1C). General analysis showed that both *Oct4* and *Nanog* expressions were higher in LAC samples than in adjacent nontumorous lung tissues by an average of 2.01-fold ($P = 0.039$) and 4.76-fold ($P = 0.029$), respectively (Fig. 1D). Approximately, 55% of the LAC samples contained an *Oct4* RNA level above that of patient-matched nontumorous lung tissues; similarly, 60% of the LAC samples contained a *Nanog* RNA level above that of patient-matched adjacent nontumorous lung tissues (Supplementary Fig. S1). Most interestingly, we observed 40% LAC cells co-overexpressed *Oct4* and *Nanog* simultaneously (Fig. 1C).

Oct4/*Nanog* overexpression enhances cancer stem-like property in LAC cells

The co-overexpression pattern of *Oct4* and *Nanog* in LAC tissues suggests a signal pathway induced by *Oct4*/*Nanog* circuit, which encourages tumorigenesis of LAC. We generated stable cell lines (A549-ON) from A549 human LAC cells using lentiviral infection system with plasmid vectors encoding *Oct4* and *Nanog* cDNA. An empty vector-transfected control (A549-Ctrl) was produced simultaneously. Interestingly, *Oct4* and *Nanog* co-overexpresion induced spindle phenotype and foci formation of A549 cells, which normally exhibit a flat brick-like morphology and hardly aggregate to each other (Fig. 2A, top left). Colonies from A549-ON cells were selected and subjected to stable clone selection. The exogenously expressed *Oct4* and *Nanog* in 3 A549-ON stable clones (Clones 1, 2, and 3) were confirmed by quantitative real-time PCR (Supplementary Figs. S2A and B) and Western Blot (Fig. 2A, bottom left). Nuclear localization of *Oct4* and *Nanog* in A549-ON cells were confirmed by immunofluorescence staining (Fig. 2A, right).

Quantitative real-time PCR analysis showed that the cancer stem-like cell marker, *CD133*, was significantly elevated in all 3 A549-ON clones, ranging from 40- to 55-fold compared to their parental A549-Ctrl cells (Fig. 2B, bottom). Flow cytometry analysis showed an increased population of *CD133*$^+$ cells in A549-ON clones (Fig. 2B, top). About 15% to 44% of the cells were determined as *CD133*$^+$ in A549-ON clones, whereas *CD133*$^+$ cells were nearly undetectable in A549-Ctrl cells. The mRNA level of another 2 stem cell–specific markers, *Mussashi-1* and *Nestin*, were also increased in A549-ON clones (Supplementary Fig. S2C and D). The elevated stem cell–specific markers suggested that A549-ON might have undergone certain process shifting cellular properties toward a state closer to stem cell or cancer stem cell.

Sphere formation and drug resistance are 2 of the important measurements used to define malignant cancers and cancer stem-like cells. In functional analyses, we found that A549-ON

DOI:10.1158/0008-5472.CAN-10-2638

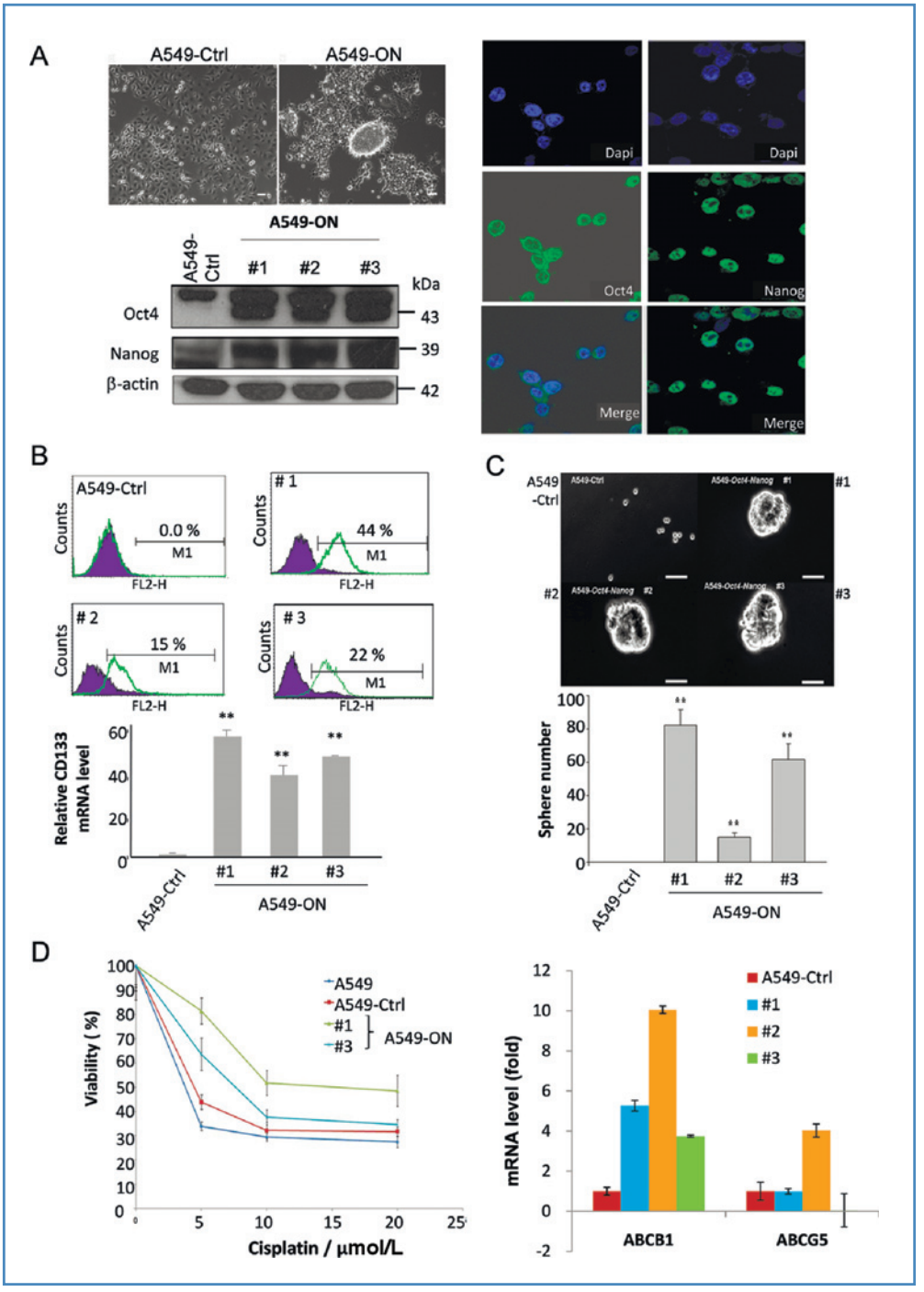

Figure 2. *Oct4*/*Nanog* overexpression enhances cancer stem-like property in LAC cell line. A, A549 cells were infected with lentiviral vectors encoding cDNA of *Oct4* and *Nanog* (A549-ON) or a control empty vector (A549-Ctrl). A549-ON cells lost the epithelial phenotype and formed foci 12 days after infection. In contrast, foci did not appear in A549-Ctrl cells. The scale bar represents a length of 50 μm (top left). A549-ON cells were subjected to stable clone selection. Three A549-ON clones (#1, #2, and #3) were analyzed by Western blot for *Oct4* and *Nanog* expression (bottom left). Immunofluorescence staining was conducted for evaluating nuclear expression of *Oct4* and *Nanog* (right). B, 3 A549-ON clones or A549-Ctrl were subjected to flow cytometry (top) and quantitative real-time PCR (bottom) to analyze the population of *CD133*$^+$ cell and *CD133* mRNA expression, respectively. C, A549-ON clones and A549-Ctrl were subjected to sphere formation assay. The sphere formation was photographed (top) and quantified (bottom). D, A549-ON clones (#1, #3), A549-Ctrl, and none transfected A549 cells (A549) were treated with cisplatin (5, 10, and 20 μmol/L) for 48 hours. The viable cells were distinguished by Trypan blue staining and counted using hemacytometer (left). A549-ON clones (#1, #2, and #3) or A549-Ctrl was subjected to quantitative real-time PCR analysis for *ABCB1* and *ABCG5* multidrug resistant gene expression (right). Data shown are the mean ± SD of 3 independent experiments.

DOI:10.1158/0008-5472.CAN-10-2638

cells have acquired the ability to form sphere in suspension culture (Fig. 2C) and were more sustainable to cisplatin treatment (Fig. 2D, left). Quantitative real-time PCR also showed that *ABCB1*, a member of the ABC family of multidrug resistant genes, was highly enhanced in all selected A549-ON clones (Fig. 2D, right).

Oct4/*Nanog* overexpression promotes *in vivo* tumorigenic and metastatic abilities of A549 cells

A549-ON clones and A549-Ctrl cells were subcutaneously injected in 8-week-old male BALB/c nude mice. Tumor growth was monitored with calipers on the days after injection as indicated (Fig. 3A). Significant increase in the growth rate of the A549-ON tumors was observed. The tumors were then surgically excised and weighed 8 weeks after injection (Fig. 3B). The tumors generated by A549-ON cells were 5- to 8-fold heavier than those by A549-Ctrl (Supplementary Fig. S3A). Interestingly, significant invasion into muscle layers was observed in hematoxylin and eosin (H&E) staining of the A549-ON tumor sections (Fig. 3C, yellow arrow heads in the top indicate muscle tissues). Compared to A549-Ctrl, a 12-fold increase of mitotic cell number in the A549-ON tumor was observed (Fig. 3C, bottom). Furthermore, staining of Alcian blue and periodic acid-Schiff (PAS), which detect mucosubstances or glycoproteins in normal lung tissue, indicated a decrease of lung-specific differentiation markers in A549-ON

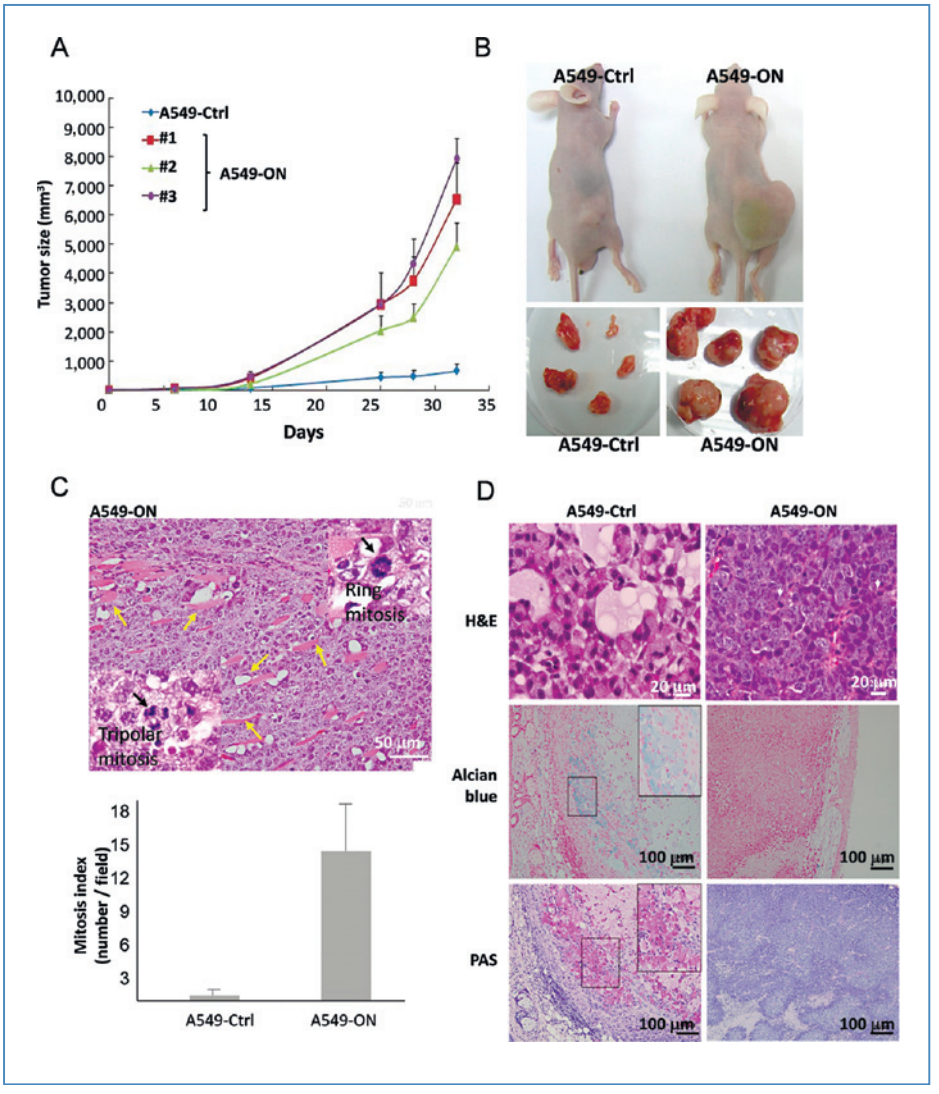

Figure 3. *Oct4/Nanog* overexpression promotes *in vivo* tumorigenic and metastatic abilities of A549-*Oct4/Nanog* cells. A, A549-ON or A549-Ctrl cells (1×10^6) were injected subcutaneously into the right or left side, respectively, of the flank region of 8-week-old male BALB/c nude mice. Tumors were measured with calipers on the days after injection as indicated. B, mice were anesthetized and sacrificed on day 42 after injection. Subcutaneous tumors were surgically excised, and the tumor size was photographed and measured. C, A549-ON tumor section was subjected to H&E staining. Significant *Oct4/Nanog* signaling-induced muscle invasion and increased cell mitosis were detected (top). Cells undergoing mitosis from A549-ON and A549-Ctrl tumors were quantified (bottom). D, the harvested tumors from A549-ON or A549-Ctrl–injected mice were paraffin embedded and subjected to H&E, Alcian blue, and PAS staining.

DOI:10.1158/0008-5472.CAN-10-2638

Table 1. Different numbers of nontransfected A549 parental cells, A549-Ctrl, A549-ON, and A549-ON cells with *Oct4*/*Nanog* double knockdown (A549-ON-shOct4+shNanog) or scrambled shRNA control (A549-ON-SC) injected in the subrenal space of nude mice

Subkidney injection (cells)	3×10^3	3×10^4	3×10^5
A549	0/3	1/3	3/3
A549-Ctrl	0/3	0/3	2/3
A549-ON	2/3	3/3	3/3
A549-ON-SC	2/3	3/3	3/3
A549-ON-shOct4+shNanog	0/3	0/3	1/3

NOTE: Experiments were performed in triplicate and the tumor formation was detected 4 weeks after injection.

tumor sections, suggesting a poorly differentiated phenotype of A549-ON cells (Fig. 3D).

A serial dilution experiment was performed to evaluate the *in vivo* tumorigenecity of A549-ON cells. Nude mice were injected with different number of cells as indicated. A549-ON, but not A549 or A549-Ctrl, generated tumors with the cell number as low as 3×10^3 cells (Table 1). Furthermore, tail vein injection experiments showed that all 3 of the A549-ON–injected mice contained metastatic lung tumors and 2 of 3 contained metastatic liver tumors, whereas only 1 A549-Ctrl–injected mice contained metastatic lung tumors and none of them contained metastatic liver tumors (Table 2).

Oct4/*Nanog*-mediated pathways regulate EMT in lung cancer cells

As EMT is associated with tumor malignancy and metastasis, we investigated the effect of *Oct4*/*Nanog* signaling on EMT process of LAC. We first observed that A549-ON cells contained a mesenchymal-like phenotype, whereas the A549-Ctrl cells stay in their original epithelial-like morphology (Fig. 4A, left). Western blotting analysis showed that the EMT-related transcription factors, *Snail* and *Slug*, and the mesenchymal markers, *Vimentin* and *N-cadherin*, were elevated in A549-ON clones, whereas the epithelial markers, *E-cadherin* and *Cytokeratin 18* (28), were suppressed (Fig. 4A, right). Functional analyses further demonstrated that A549-ON cells exhibited higher mobility and less dependence on anchorage for their growth, respectively, compared to A549-Ctrl cells (Fig. 4B).

We generated *Oct4*/*Nanog* double knockdown cells (A549-ON-shOct4+shNanog) from the previously established A549-ON cells using shRNA approach to examine the effect of *Oct4*/*Nanog* signaling on EMT. A randomly scrambled shRNA-transfected control (A549-ON-SC) was established simultaneously. The knockdown efficiency was confirmed by both quantitative real-time PCR (Fig. 4C) and Western blot (Supplementary Fig. S3B). The mRNA level of stem cell–specific marker, *CD133*, and EMT-related transcription factor, *Slug*, were reduced upon *Oct4*/*Nanog* double knockdown (Fig. 4C, left). A reduced protein level of *Snail* and *Slug*, and the elevation of *E-cadherin* and *Cytokeratin* 18 were also observed in the A549-ON-shOct4+shNanog cells (Fig. 4C, right). Moreover, *Oct4*/*Nanog* silencing was found to suppress anchorage-independent cell growth and cell migration and decrease sphere formation ability of A549-ON cells (Fig. 4D).

Knockdown of *Oct4*/*Nanog* signaling in A549-ON cell retards its tumorigenecity and mobility

Subrenal injections were performed by transplanting 3×10^3, 3×10^4, or 3×10^5 of A549-ON-shOct4+shNanog or A549-ON-SC cells in nude mice. As shown in Table 1, the tumorigenicity of A549-ON-shOct4+shNanog cells was significantly weaker than that of A549-ON-SC cells. The A549-ON-shOct4+shNanog–injected mice generated tumors only when transplanted with 3×10^5 cells or more (Table 1). A tail vein injection experiment was then conducted with A549-ON-shOct4+shNanog or A549-ON-SC cells. The metastatic tendency to lung or liver in A549-ON cells was prominently blocked by the double knockdown of *Oct4* and *Nanog* (Table 2). Moreover, the number of tumor nodules and tumor volume in lung of the transplanted mice were measured by *ex vivo* H&E

Table 2. Tail vein injection performed with 3×10^5 of each cell line

Tail vein (3×10^5)	Lung	Liver
A549	2/3	0/3
A549-Ctrl	1/3	0/3
A549-ON	3/3	2/3
A549-ON-SC	3/3	2/3
A549-ON-shOct4+shNanog	1/3	0/3

NOTE: Mice were sacrificed 6 weeks after injection and the metastases to lung or liver were examined.

DOI:10.1158/0008-5472.CAN-10-2638

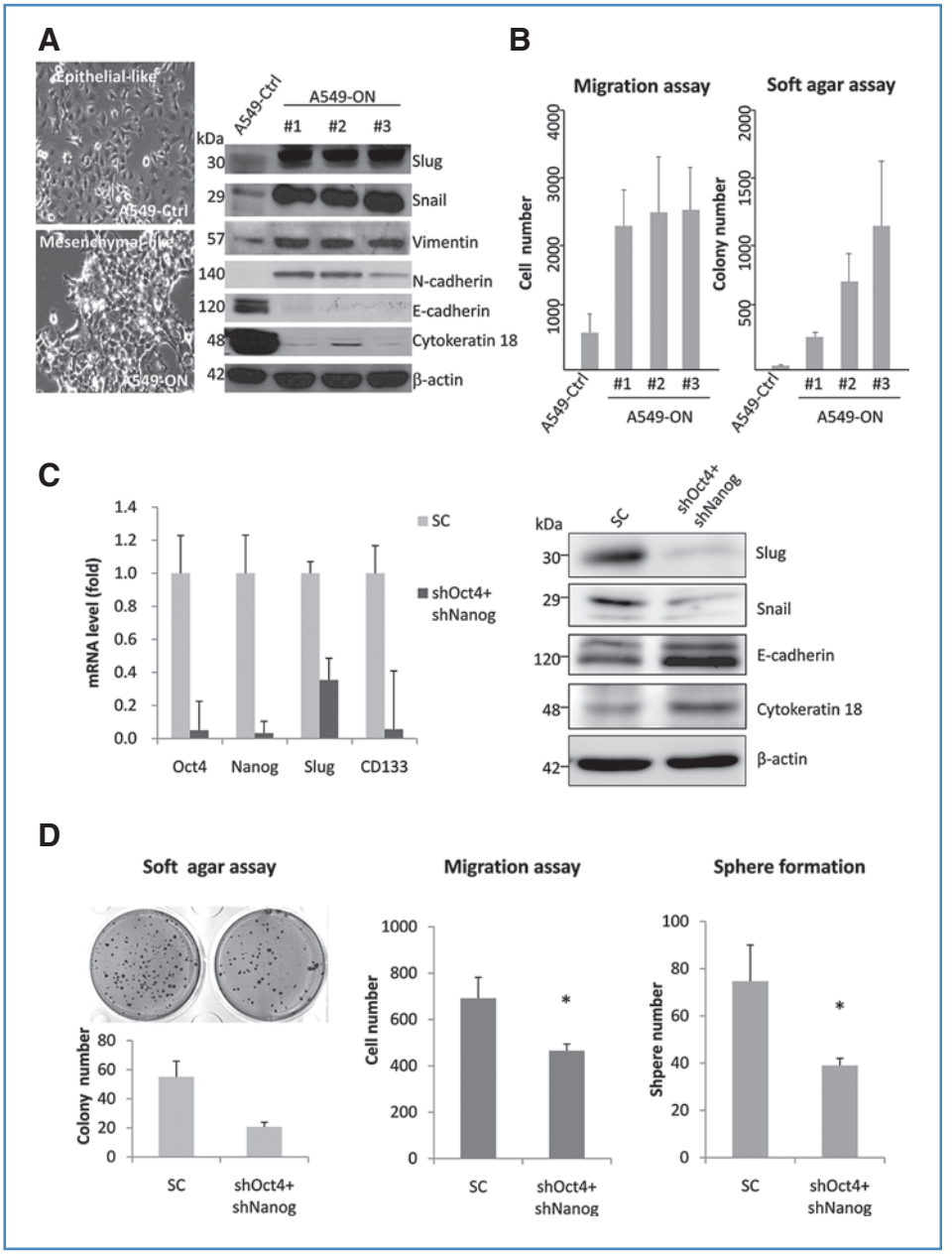

Figure 4. *Oct4*/*Nanog*-mediated pathways regulate EMT in lung cancer cells. A, the morphology of A549-ON clones and A549-Ctrl was investigated under microscope (left). Total protein of 3 A549-ON clones and A549-Ctrl was extracted and analyzed by Western blot using specific antibodies (right). B, 3 A549-ON clones and A549-Ctrl cells were subjected to TransWell cell migration assay (left) and soft agar colony formation assay (right). C, knockdown of *Oct4* and *Nanog* (shOct4+shNanog) in A549-ON clones was performed by lentiviral infection system using vectors encoding shRNA against *Oct4* and *Nanog*. A randomly scrambled shRNA control (SC) was used as an internal control. A quantitative real-time PCR analysis was conducted to assess the mRNA level of stemness genes as indicated (left). The protein levels of EMT markers were determined by Western blot (right). D, *Oct4* and *Nanog* double knockdown (shOct4+shNanog) and the scramble control (SC) cells were subjected to soft agar, migration, and sphere formation assays. Data shown are the mean ± SD of 3 independent experiments.

staining (Fig. 5A). In comparison to A549-ON cells, double knockdown of *Oct4* and *Nanog* reduced the number of metastatic nodules and size of tumor by more than 5-fold (Fig. 5B). Furthermore, mice transplanted with the A549-ON-shOct4+shNanog cells had a significantly prolonged mean survival rate compared to those implanted with A549-ON-SC or the A549-ON cells ($P < 0.05$; Fig. 5C).

Poor overall survival rate of patients with LAC was positively associated with *Oct4*, *Nanog*, and *Slug* expression

We studied the levels of *Oct4*, *Nanog*, and *Slug* proteins by immunohistochemical staining of a panel of specimens from 118 patients with LAC (Fig. 6A). Patient characteristics are summarized in Supplementary Table S3. The elevated

DOI:10.1158/0008-5472.CAN-10-2638

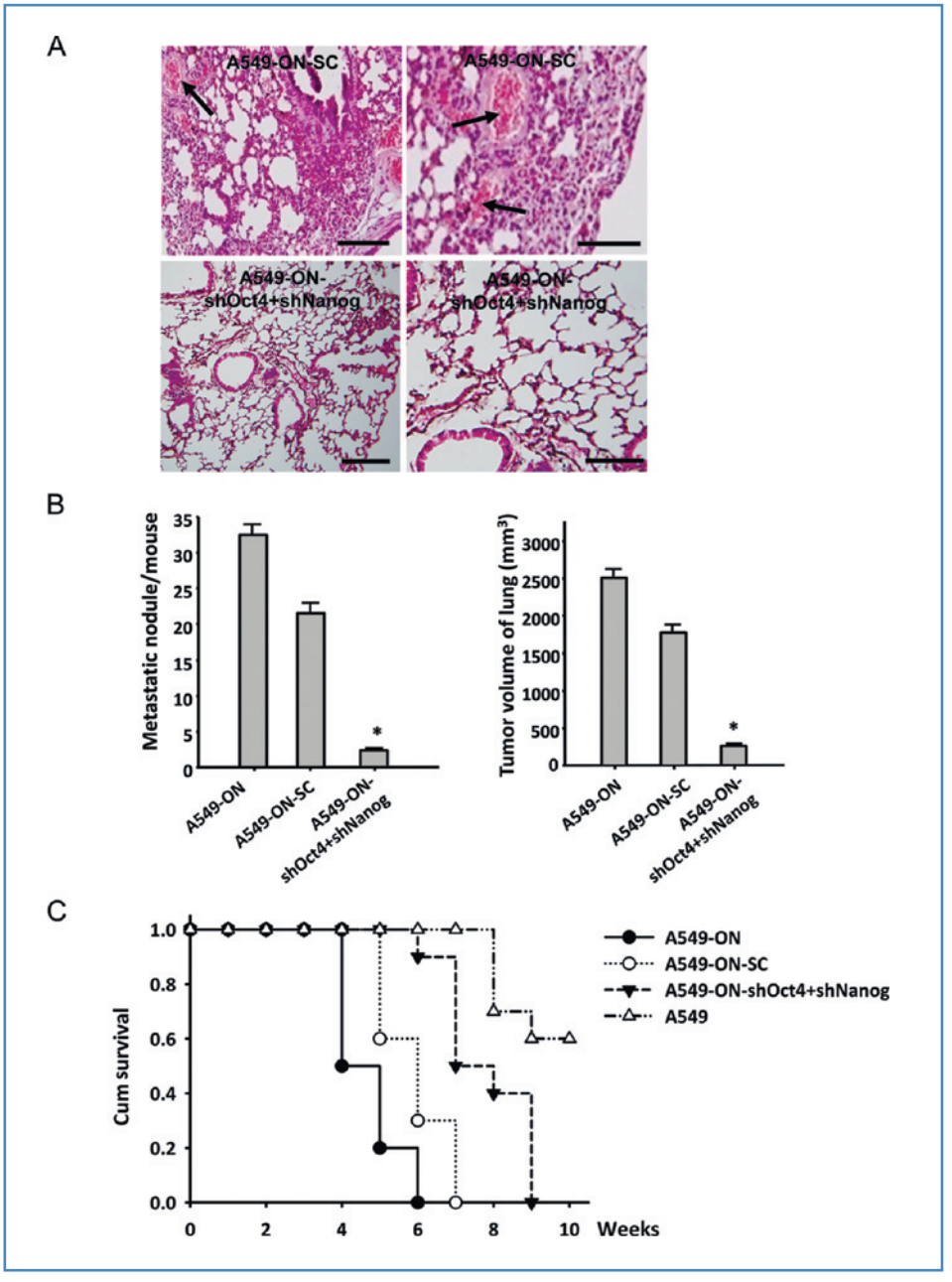

Figure 5. Double knockdown of *Oct4*/*Nanog* decreased the *in vivo* tumorigenicity of A549-ON cells and prolonged the survival time of xenotransplanted mice. A, the total volume of tumors in the lungs of mice were analyzed by histologic examination (Arrows, neovascularity and thrombosis). B, Double knockdown of *Oct4*/*Nanog* in A549-ON effectively reduced the number of metastatic tumor nodule in lung and tumor size in transplanted mice (*, $P < 0.01$). Data shown are the mean ± SD of 3 experiments. C, Kaplan–Meier survival analysis further indicated that the mean survival rate for animals receiving A549-ON-shOct4+shNanog cells was significantly prolonged compared to those receiving A549-ON-SC or A549-ON cells.

expressions of *Oct4*, *Nanog*, or *Slug* were positively associated with high-grade LAC with moderate to poor differentiation (Fig. 6A). Kaplan–Meier survival analysis was then conducted to determine the prognostic significance of *Oct4*, *Nanog*, or *Slug* expression in patients with LAC. First, the results showed that the *Oct4*-positive cases were associated with a considerably worse overall survival rate compared with *Oct4*-negative ones (Fig. 6B; $P < 0.05$). Second, patients with lower *Nanog* expression had a better survival prognosis than the *Nanog* highly expressing patients (Fig. 6B; $P < 0.01$). Third, $Slug^+$ patients had a worse survival prognosis (Fig. 6B; $P < 0.01$). Finally, patients positive for all 3 molecules ($Oct4^+Nanog^+Slug^+$) had the worst survival rate compared to other LAC patients (Fig. 6C; group 4 vs. other groups), whereas the triple negative for *Oct4*, *Nanog*, and *Slug* had the most favorable survival as compared with other groups (Fig. 6C; group 1 vs. other groups). The correlation

DOI:10.1158/0008-5472.CAN-10-2638

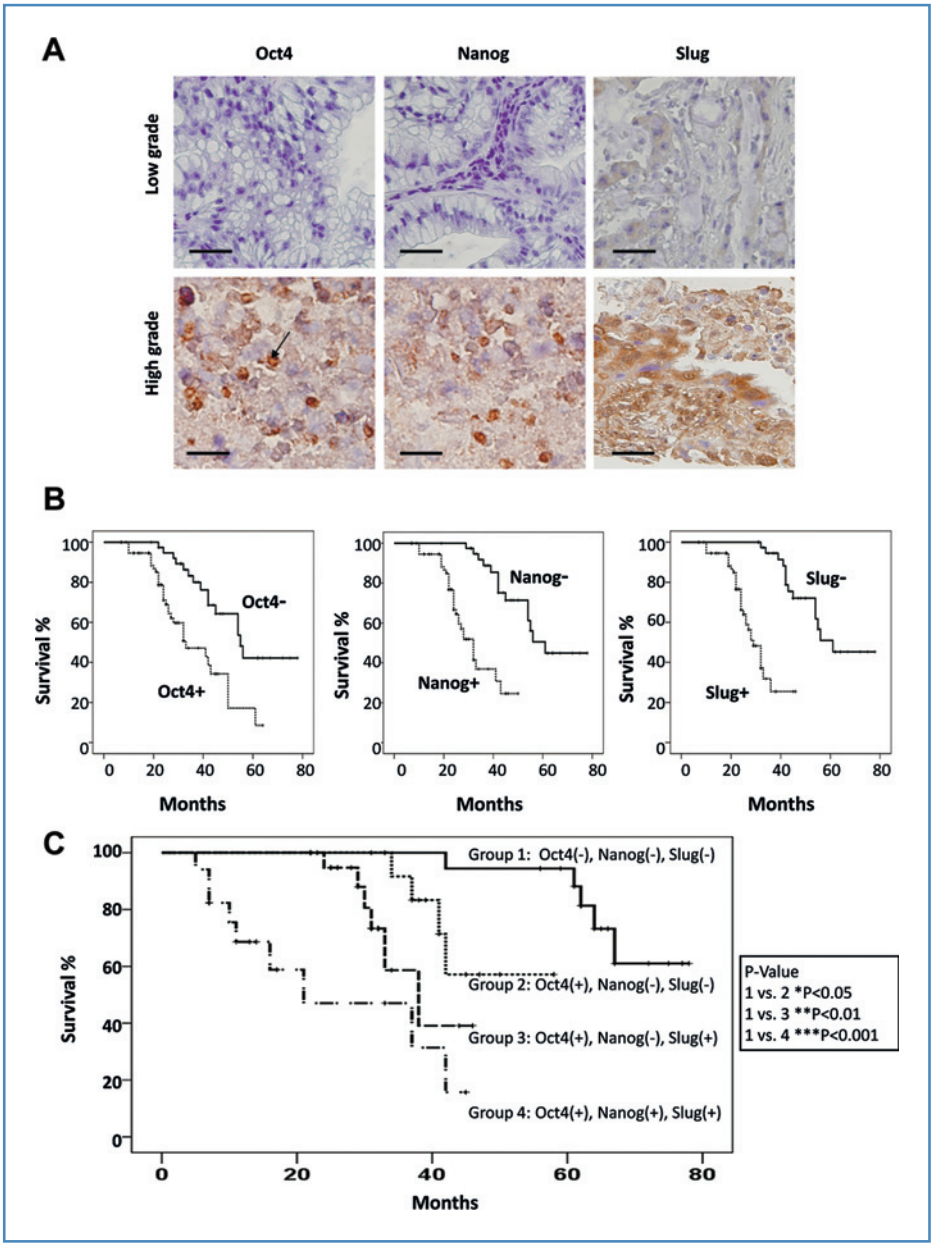

Figure 6. Correlation of *Oct4, Nanog,* and *Slug* expressions to the clinical grading and survival rate of LAC patients. A, representative results of immunohistochemical staining for *Oct4*, *Nanog*, and *Slug* in 118 LAC patients at different grades (top, low-grade; bottom, high-grade). B, Kaplan–Meier analysis of overall survival in 118 LAC patients according to single *Oct4* expression (left; *, $P < 0.01$), single *Nanog* expression (middle; **, $P < 0.01$), single *Slug* expression (right; *, $P < 0.01$), and C, the mean survival times of 118 patients with LAC in the different combination of these 3 markers of *Oct4*, *Nanog*, and *Slug* were measured by Kaplan–Meier analysis. The combined expression of triple positivity for $Oct4^+Nanog^+Slug^+$ presents the worse prediction for the patient's survival outcome (***, $P < 0.0001$). Inset box, group 1 ($Oct4^-$, $Nanog^-$, and $Slug^-$ cells) was used as the reference for comparison with other groups (2–4).

between *Oct4/Nanog/Slug* level and LAC patient survival rate may provide a novel index for predicting the disease progression and clinical outcome.

Discussion

Aberrant upregulation of EMT transcriptional factors, *Twist, Snail,* and *Slug*, is associated with poor overall and metastasis-free survival in patients with non–small cell lung cancer (29). However, upstream regulatory pathways leading to EMT-related metastasis in lung cancer remain unclear. It has been shown that poorly differentiated tumors preferentially overexpress genes normally enriched in ESCs, and downstream targets of *Oct4* and *Nanog* are more frequently overexpressed in poorly differentiated tumors than in well-differentiated ones (14, 20, 30–34).

DOI:10.1158/0008-5472.CAN-10-2638

In the present study, we demonstrated that *Oct4* and *Nanog* are significantly upregulated in LAC patients (Figs. 1 and 6). The bioinformatics and quantitative real-time PCR analysis identified that both *Oct4* and *Nanog* are co-overexpressed in LAC (Fig. 1). Ectopic coexpression of *Oct4* and *Nanog* converted A549 cells to a mesenchymal-like phenotype. Moreover, there is evidence to support that *Oct4* and *Nanog* encourage the malignancy of lung cancer cells. First of all, A549-ON cells exhibit enhanced sphere formation ability, elevated anchorage-independent growth, and increased mobility (Figs. 2 and 4). Second, A549-ON cells are highly tumorigenic and metastatic, and this is reversed by *Oct4*/*Nanog* silencing in transplanted mice (Figs. 3 and 5; Tables 1 and 2). Third, immunohistochemical analysis showed that xenograft A549-ON tumor exhibits poorly differentiated and fast mitotic phenomenon (Fig. 3). Finally and most importantly, ectopically overexpressed *Oct4*/*Nanog* elevates mesenchymal markers and suppresses epithelial markers (Fig. 4). We propose that *Oct4*/*Nanog* might positively regulate tumor metastasis through enhancing EMT in LAC.

We have shown that *Slug* is a possible target for *Oct4* and *Nanog* and exerts their effect on the regulation of EMT. The mRNA and protein levels of *Slug* are increased upon *Oct4*/*Nanog* overexpression and decreased by RNAi-mediated *Oct4*/*Nanog* knockdown (Fig. 4). The reporter assay further supported the regulatory role of *Oct4*/*Nanog* signaling on *Slug* promoter (Supplementary Fig. S4). Because *Oct4* binds *Nanog* to activate gene expression in ESCs (35), it is possible that *Oct4* and *Nanog* work together in their target genes to induce EMT. Further characterizations are required to illustrate how *Oct4* and *Nanog* regulate *Slug* or other EMT-related factors, if any.

Lung cancer is notorious for its difficult diagnosis at early stage and poor recurrence-free prognosis. Advanced diagnostic methods and novel prognosis markers are urgently needed to improve the clinical treatments of the disease. The studies on hepatocellular carcinoma (HCC) proposed that *Oct4* mRNA might be a biomarker for assessing the prognosis of HCC (32). Recently, the elegant study by Bass and colleagues (36) demonstrated that the DNA copy numbers of Sox2 were highly amplified in lung and esophageal squamous cell carcinomas. A detailed analysis done by Hassan and colleagues (31) has demonstrated that the expression profile of ESC-like genes, including overlapped targets of *Oct4*, *Nanog*, and *Sox2*, is preferentially detected in histologically poorly differentiated LAC, but not lung squamous cell carcinoma, suggesting that ESC genes may be involved in prognosis of LAC. In line with their findings, our data further showed that the expression levels of *Oct4*, *Nanog*, and *Slug*, individually or simultaneously, are oppositely correlated with the 5-year survival rate of LAC patients (Fig. 6). The clinical significance of *Oct4/Nanog/Slug* would be worth exploring in the future.

In conclusion, the present study has demonstrated that *Oct4* and *Nanog* induce cancer stem cell–like properties and enhance EMT, contributing to the tumorigenesis and metastasis in LAC. The *Oct4*/*Nanog*-induced EMT could be regulated partly, if not fully, via increasing *Slug* transcription. Moreover, we have shown a correlation between the worse prognosis of LAC patients and the high expression of *Oct4/Nanog/Slug*. We propose that the *Oct4/Nanog/Slug* would be a potential marker of prognosis and a novel target of therapy for LAC.

Disclosure of Potential Conflicts of Interest

No potential conflicts of interest were disclosed.

Grant Support

This research was supported by the Institute of Biomedical Sciences, Academia Sinica, the National Yang-Ming University, the Department of Health (DOH97-TD-G-111-023; DOH99-TD-C-111-007), and National Science Council (NSC97-3111-B-010-005; 97-3111-B-075-001-MY3), Executive Yuan, Taiwan, R.O.C.

The costs of publication of this article were defrayed in part by the payment of page charges. This article must therefore be hereby marked *advertisement* in accordance with 18 U.S.C. Section 1734 solely to indicate this fact.

Received 07/20/2010; revised 10/12/2010; accepted 10/15/2010; published Online 12/15/2010.

References

1. Spira A, Ettinger DS. Multidisciplinary management of lung cancer. N Engl J Med 2004;350:379–92.
2. Lam WK, Watkins DN. Lung cancer: future directions. Respirology 2007;12:471–7.
3. Boiani M, Scholer HR. Regulatory networks in embryo-derived pluripotent stem cells. Nat Rev Mol Cell Biol 2005;6:872–84.
4. Nichols J, Zevnik B, Anastassiadis K, Niwa H, Klewe-Nebenius D, Chambers I, et al. Formation of pluripotent stem cells in the mammalian embryo depends on the POU transcription factor Oct4. Cell 1998;95:379–91.
5. Pesce M, Wang X, Wolgemuth DJ, Scholer H. Differential expression of the Oct-4 transcription factor during mouse germ cell differentiation. Mech Dev 1998;71:89–98.
6. Chambers I, Colby D, Robertson M, Nichols J, Lee S, Tweedie S, et al. Functional expression cloning of Nanog, a pluripotency sustaining factor in embryonic stem cells. Cell 2003;113:643–55.
7. Cavaleri F, Scholer HR. Nanog: a new recruit to the embryonic stem cell orchestra. Cell 2003;113:551–2.
8. Okita K, Ichisaka T, Yamanaka S. Generation of germline-competent induced pluripotent stem cells. Nature 2007;448:313–7.
9. Park IH, Zhao R, West JA, Yabuuchi A, Huo H, Ince TA, et al. Reprogramming of human somatic cells to pluripotency with defined factors. Nature 2008;451:141–6.
10. Yu J, Vodyanik MA, Smuga-Otto K, Antosiewicz-Bourget J, Frane JL, Tian S, et al. Induced pluripotent stem cell lines derived from human somatic cells. Science 2007;318:1917–20.
11. Ling TY, Kuo MD, Li CL, Yu AL, Huang YH, Wu TJ, et al. Identification of pulmonary Oct-4+ stem/progenitor cells and demonstration of their susceptibility to SARS coronavirus (SARS-CoV) infection *in vitro*. Proc Natl Acad Sci U S A 2006;103:9530–5.
12. Chen YC, Hsu HS, Chen YW, Tsai TH, How CK, Wang CY, et al. Oct-4 expression maintained cancer stem-like properties in lung cancer-derived CD133-positive cells. PLoS One 2008;3:e2637.
13. Ponti D, Costa A, Zaffaroni N, Pratesi G, Petrangolini G, Coradini D, et al. Isolation and *in vitro* propagation of tumorigenic breast cancer cells with stem/progenitor cell properties. Cancer Res 2005;65:5506–11.
14. Meng HM, Zheng P, Wang XY, Liu C, Sui HM, Wu SJ, et al. Over-expression of nanog predicts tumor progression and poor prognosis in colorectal cancer. Cancer Biol Ther 2010 [Epub ahead of print].

DOI:10.1158/0008-5472.CAN-10-2638

15. Gidekel S, Pizov G, Bergman Y, Pikarsky E. Oct-3/4 is a dose-dependent oncogenic fate determinant. Cancer Cell 2003;4:361–70.
16. Jin T, Branch DR, Zhang X, Qi S, Youngson B, Goss PE. Examination of POU homeobox gene expression in human breast cancer cells. Int J Cancer 1999;81:104–12.
17. Monk M, Holding C. Human embryonic genes re-expressed in cancer cells. Oncogene 2001;20:8085–91.
18. Wang P, Branch DR, Bali M, Schultz GA, Goss PE, Jin T. The POU homeodomain protein OCT3 as a potential transcriptional activator for fibroblast growth factor-4 (FGF-4) in human breast cancer cells. Biochem J 2003;375:199–205.
19. Wen J, Park JY, Park KH, Chung HW, Bang S, Park SW, et al. Oct4 and Nanog expression is associated with early stages of pancreatic carcinogenesis. Pancreas 2010;39:622–6.
20. Chiou SH, Yu CC, Huang CY, Lin SC, Liu CJ, Tsai TH, et al. Positive correlations of Oct-4 and Nanog in oral cancer stem-like cells and high-grade oral squamous cell carcinoma. Clin Cancer Res 2008;14:4085–95.
21. Acloque H, Adams MS, Fishwick K, Bronner-Fraser M, Nieto MA. Epithelial-mesenchymal transitions: the importance of changing cell state in development and disease. J Clin Invest 2009;119:1438–49.
22. Kalluri R. EMT: when epithelial cells decide to become mesenchymal-like cells. J Clin Invest 2009;119:1417–9.
23. Mani SA, Guo W, Liao MJ, Eaton EN, Ayyanan A, Zhou AY, et al. The epithelial-mesenchymal transition generates cells with properties of stem cells. Cell 2008;133:704–15.
24. Hong CF, Chou YT, Lin YS, Wu CW. MAD2B, a novel TCF4-binding protein, modulates TCF4-mediated epithelial-mesenchymal transdifferentiation. J Biol Chem 2009;284:19613–22.
25. Chiou SH, Chen SJ, Chang YL, Chen YC, Li HY, Chen DT, et al. MafA promotes the reprogramming of placenta-derived multipotent stem cells into pancreatic islets-like and insulin-positive cells. J Cell Mol Med 2010 [Epub ahead of print].
26. Jordan CT, Guzman ML, Noble M. Cancer stem cells. N Engl J Med 2006;355:1253–61.
27. Eramo A, Lotti F, Sette G, Pilozzi E , Biffoni M , Di Virgilio A , et al. Identification and expansion of the tumorigenic lung cancer stem cell population. Cell Death Differ 2008;15:504–14.
28. Kolosionek E, Savai R, Ghofrani HA, Weissmann N, Guenther A, Grimminger F, et al. Expression and activity of phosphodiesterase isoforms during epithelial mesenchymal transition: the role of phosphodiesterase 4. Mol Biol Cell 2009;20:4751–65.
29. Wang SP, Wang WL, Chang YL, Wu CT, Chao YC, Kao SH, et al. p53 controls cancer cell invasion by inducing the MDM2-mediated degradation of Slug. Nat Cell Biol 2009;11:694–704.
30. Ben-Porath I, Thomson MW, Carey VJ, Ge R, Bell GW, Regev A, et al. An embryonic stem cell-like gene expression signature in poorly differentiated aggressive human tumors. Nat Genet 2008;40:499–507.
31. Hassan KA, Chen G, Kalemkerian GP, Wicha MS, Beer DG. An embryonic stem cell-like signature identifies poorly differentiated lung adenocarcinoma but not squamous cell carcinoma. Clin Cancer Res 2009;15:6386–90.
32. Huang PZ, Lu CL, Li BK, Hong J, Huang L, Wang L, et al. OCT4 expression in hepatocellular carcinoma and its clinical significance. Ai Zheng 2010;29:105–9.
33. Rody A, Karn T, Ruckhaeberle E, Hanker L, Gaetje R, Holtrich U, et al. Differentially expressed genes of reprogrammed human pluripotent stem cells in breast cancer. Eur J Cancer 2008;44:1789–92.
34. Wong DJ, Liu H, Ridky TW, Cassarino D, Segal E, Chang HY. Module map of stem cell genes guides creation of epithelial cancer stem cells. Cell Stem Cell 2008;2:333–44.
35. Liang J, Wan M, Zhang Y, Gu P, Xin H, Jung SY, et al. Nanog and Oct4 associate with unique transcriptional repression complexes in embryonic stem cells. Nat Cell Biol 2008;10:731–9.
36. Bass AJ, Watanabe H, Mermel CH, Yu S, Perner S, Verhaak RG, et al. SOX2 is an amplified lineage-survival oncogene in lung and esophageal squamous cell carcinomas. Nat Genet 2009;41:1238–42.